Proceedings of the ASME 2010 3rd Joint US-European Fluids Engineering Summer Meeting and 8th International Conference on Nanochannels, Microchannels, and Minichannels
FEDSM-ICNMM2010
August 1-5, 2010, Montreal, Canada

FEDSM-ICNMM2010-30887

INVESTIGATION OF SIDE-VIEW MIRROR FLOW-INDUCED VIBRATION PHENOMENA

Mehmet N. Tomac
The Ohio State University
Columbus, OH, USA

Kevin Yugulis
The Ohio State University
Columbus, OH, USA

James W. Gregory
The Ohio State University
Columbus, OH, USA

ABSTRACT

The primary objective of this research is to develop an understanding of the flow mechanisms which induce side-view mirror vibrations. The unsteady nature of the flow over side-view mirrors causes unsteady aerodynamic load distributions and flow-induced vibrations on the mirror assembly. These vibrations generate blurred rear-view images and higher noise levels, affecting the safety and comfort of the passengers. Geometrical design features of side-view mirrors exacerbate the flow-induced vibration levels of the mirror assembly significantly. This work quantifies the impact of these design features on the vibration amplitude; develops a methodology for testing mirror vibrations in a small, low-speed wind tunnel using only the mirror of interest; and delves into the interactions between the bluff body mirror geometry and its wake. Two similar side-view mirror designs, a baseline design and a turn-signal design, were investigated. The baseline mirror has a sharp-edged corner near the trailing edge, while the turn-signal design has an edge with an increased radius of curvature for the tip profile. A laser-based vibration measurement technique was developed and used to quantify vibration levels. Flow visualization, Particle Image Velocimetry (PIV), Constant Temperature Anemometry (CTA), and Surface Stress Sensitive Film (S^3F) techniques were used to understand the separation characteristics over the mirrors since the time-dependent changes in separation location directly affect the unsteady loading on the mirror. The flow over the turn signal mirror with larger tip radius has larger excursions in the separation location, a wider wake, increased unsteadiness, and higher vibration levels. Results at the high Reynolds numbers for these test conditions indicate the absence of a discrete vortex shedding frequency. However, vortical structures in the wake are correlated with unsteady movement of the separation location.

INTRODUCTION

Flows over bluff bodies are often encountered in engineering applications. As the fluid flows over a bluff body, flow separates and vortex shedding occurs with a particular frequency proportional to the fluid velocity. The periodic nature of the vortex shedding disappears and flow exhibits an unsteady vortex shedding as the Reynolds number (Re) exceeds a critical value depending on the geometry of the bluff body. Achenbach[1] studied vortex shedding over spheres by using hot-wire anemometry. Achenbach could not detect any periodic vortex shedding frequency beyond a critical Reynolds number of 3.7×10^5. This non-periodic and unsteady behavior of the vortex shedding causes instabilities in the flow and due to these instabilities the time-averaged separation location moves continually. This type of flow condition imposes unsteady loading on the body and causes structural vibrations (flow-induced vibrations). With increased velocity, these vibrations reach a point where they are no longer acceptable in terms of design expectations. A review of the literature indicates that designers have experienced the problem of flow-induced vibration on side view mirrors. Watkins[2] performed wake surveys of a mirror housing and instrumented the mirror with miniature accelerometers. Watkins found that aerodynamic forcing inputs were the significant driving force in mirror vibration studies in both wind tunnel and road testing. The typical mirror vibration angles measured in Watkins' investigation ranged from 1 to 3 arc minutes, with the vibration modes exhibiting a preferential axis. The magnitude of vibrations measured in wind tunnel testing was found to be roughly equivalent to magnitudes measured in road tests. Horinouchi et al.[3] studied the forcing of mirror vibration through PIV and CFD studies. Horinouchi's results indicate that the vibration imparted to the mirror surface by airflow excites the natural vibration mode of the mirror surface, thereby causing the mirror to vibrate. Homsi[4] performed an early CFD study to illustrate the correlation between vortex shedding and mirror vibration.

In this study, flow induced vibrations on side view mirrors were investigated. The working hypothesis of this study is that mirror vibrations are caused by unsteady forcing on the mirror housing due to an oscillating separation location and unsteady vortex generation. This hypothesis was investigated through a range of measurement techniques to correlate unsteady vortex shedding in the wake with the mirror vibrations. A comparison between two different side view mirror designs was accomplished in terms of flow induced vibration characteristics.

EXPERIMENTAL SETUP

This experimental study was conducted in the Ohio State University 3'x5' open-loop subsonic wind tunnel. A turn-signal mirror (TS) with a curved lens mounted at the tip was compared with a baseline geometry which had a sharp edge across the tip of the mirror housing (see Figure 1 and Figure 2). In order to ensure that mass and damping properties were held constant in this comparative study, one mirror assembly was tested with only the detail of the tip geometry being changed. A turn-signal mirror (TS) was tested in original production form, and subsequently modified with a piece of clay in order to represent the baseline mirror (BL). This geometric modification isolates the influence of tip shape from all other experimental variables. By doing this, the mass and stiffness values were held constant and the only difference is the geometry of the tip region. Figure 1 shows the baseline and the turn signal configurations tested in the experiments and Figure 2 shows the cross-sections of both designs. The mirror assembly measures approximately 0.254m long, 0.165m wide, and 0.076m thick.

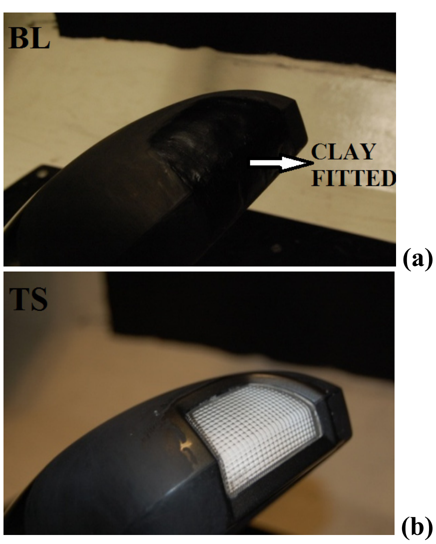

Figure 1
The baseline mirror (a) and the turn signal mirror (b)

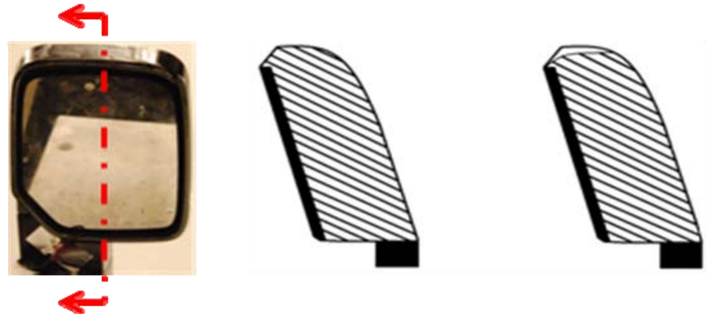

Figure 2
Cross sections of the mirrors
Baseline (left) - Turn Signal (right)

A fixture based on a NACA 0025 profile was built in order to mount the mirrors in the wind tunnel test section as shown in Figure 3. Flow visualizations were performed to determine the effect of the fixture on flow. This fixture was tested without a mirror assembly installed and the results did not show significant flow disturbances. In order to best match the flow conditions experienced by the vehicle-mounted mirror, the mounting angle was selected with the help of full-vehicle time-averaged CFD simulations. Several attachment fixtures were fabricated to set the angle of the mirror relative to the flow in discrete increments. The three selected angles between the rear face of the mirror and a vertical plane were set at 33°, 36°, or 39°. The results presented in this paper belong to the 39° pitch angle. While it is possible to match the overall flow angle, gradients in flow angularity or velocity, as well as flow unsteadiness, are impossible to match in this wind tunnel environment.

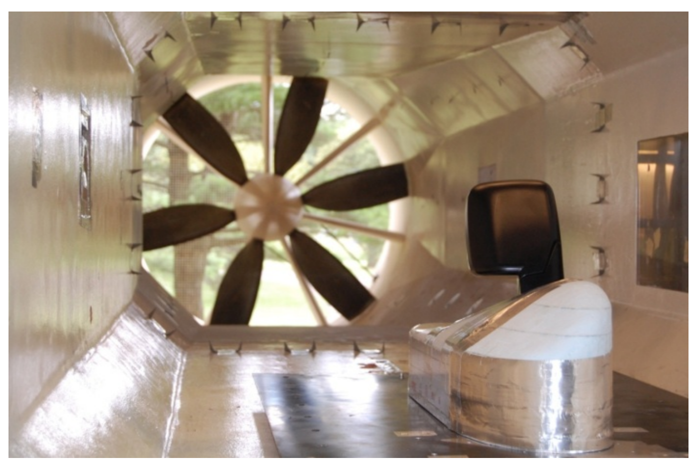

Figure 3
Mounting of the side view mirror looking downstream

A laser-based measurement technique was developed for vibration measurements and a schematic of this technique is shown in Figure 4. The laser system provides real time plots for visual analysis and vibration data for post-processing analysis. The system is comprised of a 20-mW HeNe laser beam reflected off the side view mirror glass and monitored by a dual-layer position-sensitive photodetector. Incident laser light on the photodetector face induces a current on a silicon resistive sheet. Two electrodes at the edges of the sheet monitor the change in current and sum the differences to find the lateral placement of the laser spot centroid on the detector. Two of these sheets, running in perpendicular directions, are used to determine the X- and Y-coordinates of the beam's centroid. The response of the photodetector voltage is linear with respect to incident laser spot position. Therefore, the mirror's vibration amplitude can be calculated by finding the displacement of the laser spot relative to the angle and distance between the mirror and the photo-detector. The X- and Y-outputs of the photodetector can be monitored real-time and recorded with data acquisition (DAQ) hardware. Displacements in the streamwise direction correspond to the displacements in the Y-coordinate of the sensor.

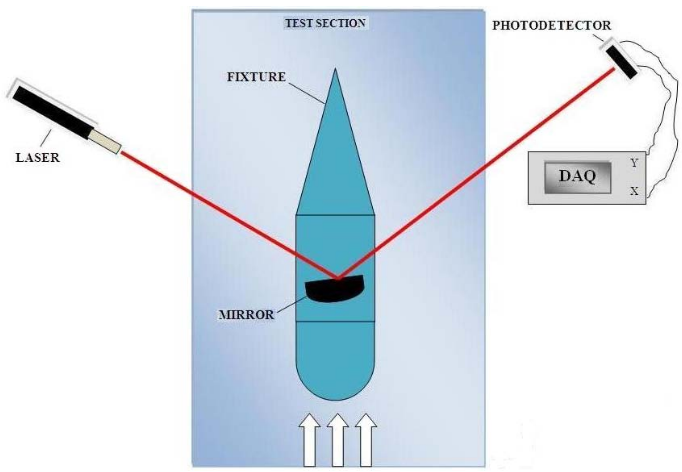

Figure 4
Schematic top view of the laser measurement setup

The laser vibration technique inherently measures the vibrations of both the mirror housing and the mirror glass simultaneously. The mirror glass could potentially vibrate at a different mode from the mirror housing in a complex manner. To investigate this possibility, independent accelerometer and laser vibration measurements were performed, as well as laser vibration measurements reflecting off a mirror securely fixed to the housing. Both sets of measurements indicated that the mirror glass and the mirror housing vibrated with the same modal characteristics. Thus, throughout the course of this investigation, vibration measurements from a laser incident on the mirror glass are considered indicative of the vibration characteristics of the mirror housing.

Flow visualization was performed by using a 200 mJ pulsed Nd:YAG green laser, a CCD camera, and a flow seeder. The camera was located perpendicular to the laser sheet, and instantaneous visualizations of the flow were obtained by synchronizing the laser and the camera. The same hardware configuration was also used for the PIV technique in order to obtain the 2D velocity field of the flow. A schematic of the system used for flow visualization and PIV is given in Figure 5.

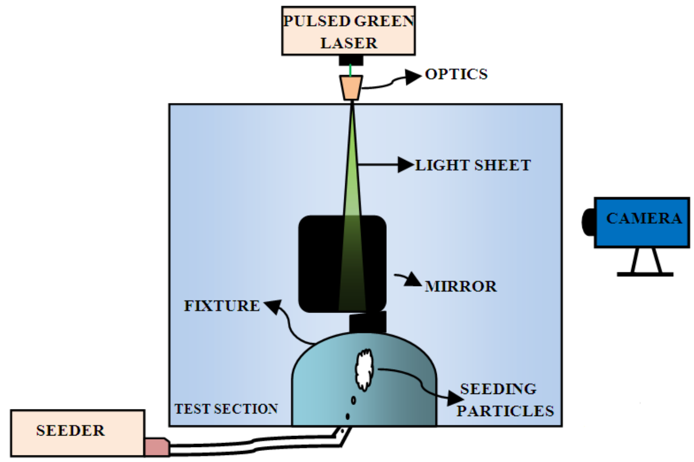

Figure 5
Schematic of the flow visualization and PIV setups

CTA measurements provide the local velocity for a given point in the flow. A TSI 1210-20 single-wire hotfilm probe with TSI 1053B anemometer and TSI 1057 signal conditioner were used for these measurements. The diameter and length of the wire are 50.8 μm and 1.02 mm, respectively. A schematic of the system is given in Figure 6. The probe was positioned throughout the flow field around the mirror by a rudimentary traverse system. Flow characteristics at locations near to and far from the surface of the mirror were explored with this system with 1-mm intervals, starting 1-mm away from the mirror surface. Measurement locations are shown in Figure 7. A Labview code was written for hotfilm probe calibration and data acquisition purposes.

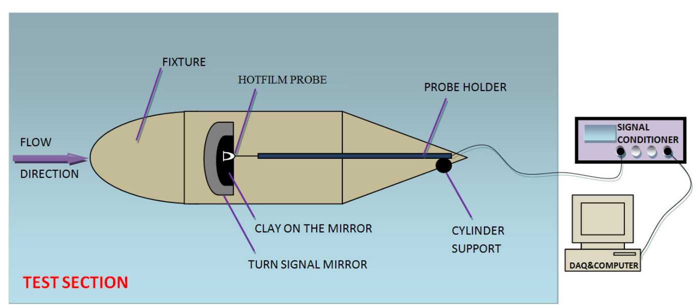

Figure 6
Schematic of the hotfilm setup in the wind tunnel

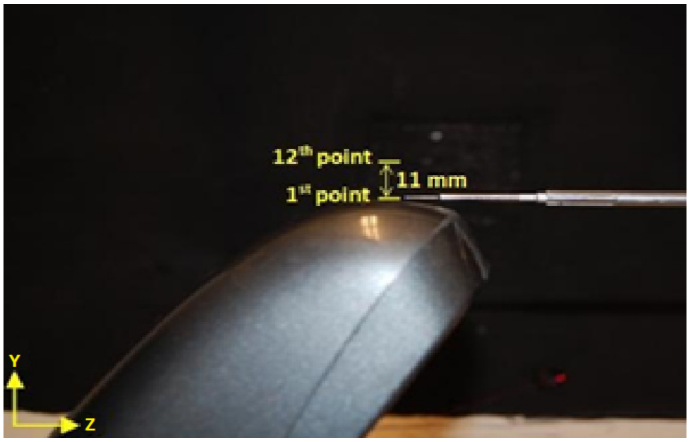

Figure 7
Measurement locations of the hotfilm probe

Surface stress sensitive film (S^3F) is a direct method to measure surface shear stress[5], shown schematically in Figure 8. The measurement technique is based on a flexible, elastomeric film applied to a surface. The properties of the film (thickness and shear modulus) are tailored such that the sensitivity of the system is tuned to the appropriate values of surface shear. The normal and tangential deformations (due to an applied shear stress and pressure field) are measured optically by tracking the tangential surface deformation via cross-correlation techniques and determining the film thickness distribution through intensity recordings. Since the effects of pressure and shear induce a coupled response on the thickness and surface deformation of the film, an FEA model of the system is used in post-processing to inversely solve for the applied pressure and surface shear stress distributions. Application of the S^3F technique to the mirror surface allows for direct determination of the separation location. A detailed description of the S^3F calibration process can be found in Reference 7.

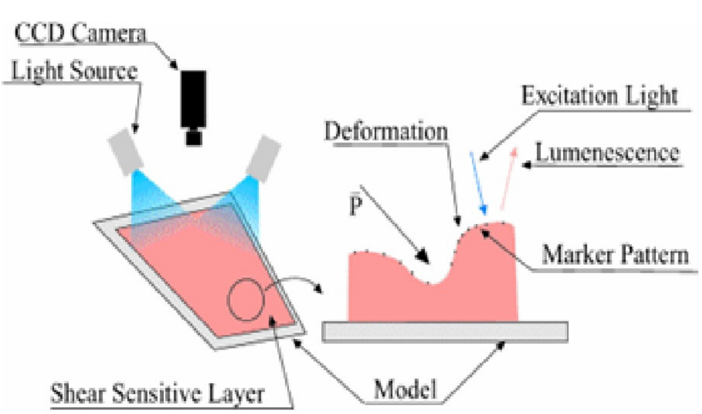

Figure 8
Schematic of S^3F technique[6]

RESULTS

Laser Measurements

Laser vibration measurements were performed over a velocity range from 25 m/s to 42 m/s (for a Reynolds number, based on mirror length, of 4.05×10^5 to 6.75×10^5). The vibration frequency was found to vary with the velocity. The most critical range for vibrations was observed to be near 42 m/s, and was selected to be the primary test condition for this investigation. Although 42 m/s (94 mi/hr) is faster than the legal speed limit on North American highways, it was selected as the primary test point due to the clarity of the results (i.e. the most significant differences between the turn signal and the baseline mirror were observed at this condition). Similar trends were exhibited throughout the velocity range. Furthermore, a side view mirror mounted on a vehicle travelling at highway speeds will experience much higher local velocity (compared to the freestream velocity) due to acceleration of the flow over the fore body and windshield of the vehicle.

Although both mirrors exhibited similar vibration frequencies, the magnitudes of the vibrations were different. The strongest vibrations were encountered at a frequency of 45 Hz in the streamwise direction (motion along the z-axis in Figure 7), when the flow induced vibration frequency was approximately equal to the natural frequency of the mirror / mounting fixture combination (for either mirror). For 42 m/s, a 10-dB difference in vibration magnitude between the turn signal mirror and the baseline mirror was measured, as shown in Figure 9. Note that the frequency peak observed at 20 Hz is a sub-harmonic at half of the fundamental frequency.

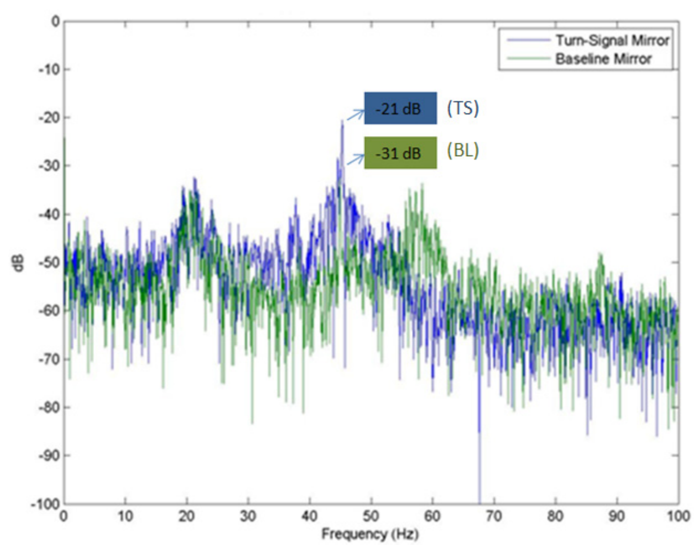

Figure 9
Power spectrum for 42 m/s

Flow Visualization

Figure 10 illustrates flow visualization along the centerline of the baseline mirror at one instant in time. The Kelvin-Helmholtz instability is clearly visible in this 2D plane, and represents a laminar separation with a turbulent wake. The separation location is over the portion of the mirror where the turn signal assembly is mounted.

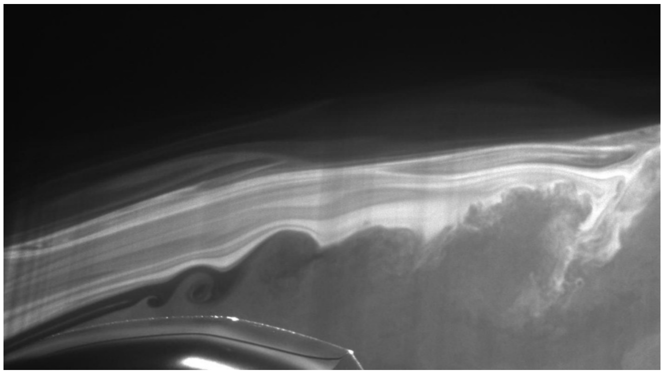

Figure 10
Instantaneous vortex structure over the baseline mirror

In order to study the temporal characteristics of the separation location, a series of images was acquired for both the baseline mirror and the turn signal mirror. Figure 11 shows consecutive images for both mirrors at a velocity of 42 m/s, acquired at a frame rate of 15 Hz (sub-sampling the fundamental frequency). The images in left column for the baseline mirror show a consistent separation location, while images in right column for the turn signal mirror show a shifting separation location which traverses the extent of the rounded turn signal assembly. This shows that the separation location oscillates much more for the turn signal mirror when compared to the baseline mirror. This difference is shown to be the cause of the increased vibration levels observed for the turn signal mirror.

Particle Image Velocimetry

In order to quantify the findings from flow visualization, PIV was used to record the velocity throughout a plane on the centerline of the mirror. Figure 12 and Figure 13 present processed images for the baseline and turn signal mirror, respectively, at 42 m/s. The separation location can be found as the point at which the vectors no longer follow the contour of the mirror surface. Note that in Figure 12, the flow separates near the front tip, while in Figure 13 the separation location is near the top of the mirror. A series of processed images for the baseline mirror show a steady and consistent separation near the tip of the mirror, while a series of images for the turn signal mirror show an oscillatory movement in the separation location. These PIV images serve to reinforce conclusions derived from the flow visualization images.

The PIV technique provides the velocity vectors for the flow field. Nevertheless, this technique is unable to provide time-resolved information about the flow physics as the sampling rate of PIV is almost an order of magnitude lower than what is required to capture the unsteadiness of the shear layer in full detail. However, CTA is a well-known technique with the ability to provide high frequency response although it can only measure velocity at a single point in the flow.

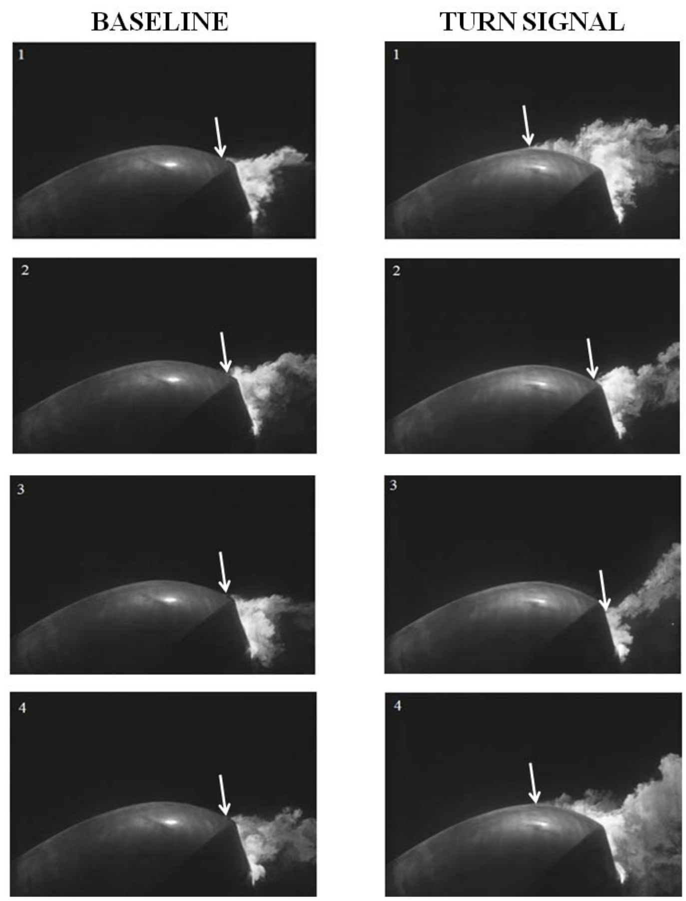

Figure 11
Consecutive flow visualization images at 42 m/s

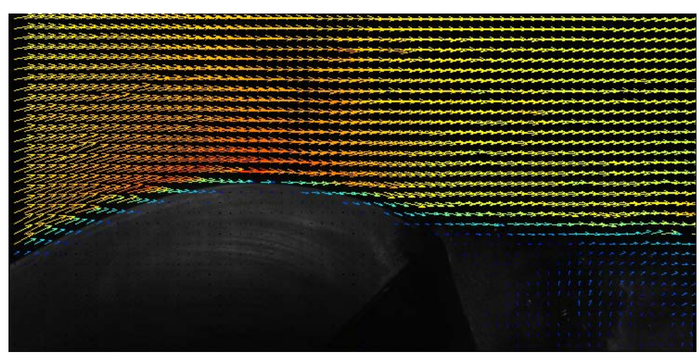

Figure 12
Velocity field over the baseline mirror at 42m/s

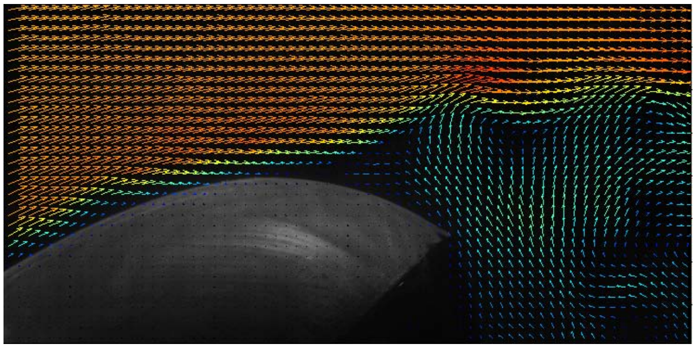

Figure 13
Velocity field over the turn signal mirror at 42m/s

Hotfilm Measurements

Hotfilm measurements were taken for a velocity range of 25 m/s to 42 m/s, where Re based on mirror length is 6.75×10^5 for 42 m/s. Velocity fluctuations on both mirrors were measured by using CTA for comparison purposes. The location of the hotfilm probe allowed measurements to be taken where high shear layer instabilities exist. The magnitude of the fluctuations is quantified by calculating the RMS of a long time record to determine the level of unsteadiness in the flow. Figure 14 shows the processed RMS values for three different freestream velocities. On these plots, RMS is plotted as a function of distance above the mirror housing tip. RMS velocity is a critical parameter to evaluate in this investigation (rather than the typical RMS fluctuations normalized by mean velocity) because it is the absolute magnitude of the velocity fluctuations that drives the mirror vibrations.

As the free-stream velocity increases, velocity fluctuations (RMS) increase for both mirrors. However, the turn signal mirror has a wider distribution of elevated RMS throughout the entire velocity range. This characteristic corresponds to increased shear layer instabilities and a larger region of unsteadiness. At a distance of 6 mm away from the mirror surface, both mirrors experience a maximum in velocity fluctuation. The velocity fluctuations around the baseline mirror appear to then dampen exponentially with distance, while they decrease rather linearly with distance for the turn signal mirror. This shows that the tip modification at the baseline mirror causes a wider and more unstable wake in addition to the shifting separation location. More specifically, the near-wake for the turn signal mirror appears to terminate around 10 mm from the clay surface level, while the near-wake from the baseline mirror terminates around 8 mm from the clay surface. Table 1 gives values for the difference in RMS of the two mirrors at three locations: 6, 7, and 8 mm above the surface. Arithmetic average of these three positions' RMS values yields a velocity fluctuation of almost 4 m/s for the case of 42 m/s. This indicates that these fluctuations play a key role in driving the flow-induced vibrations on the mirror housing.

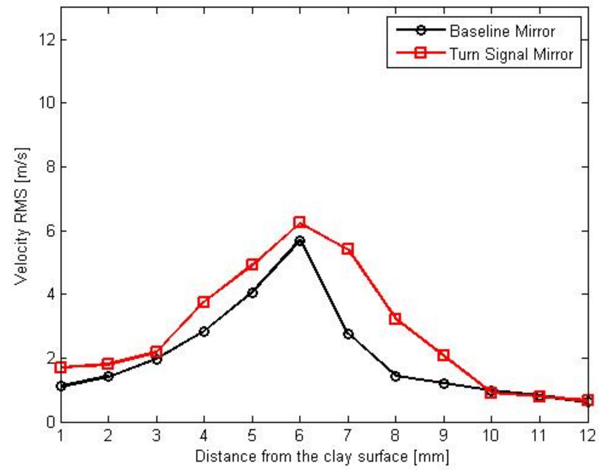

(a)

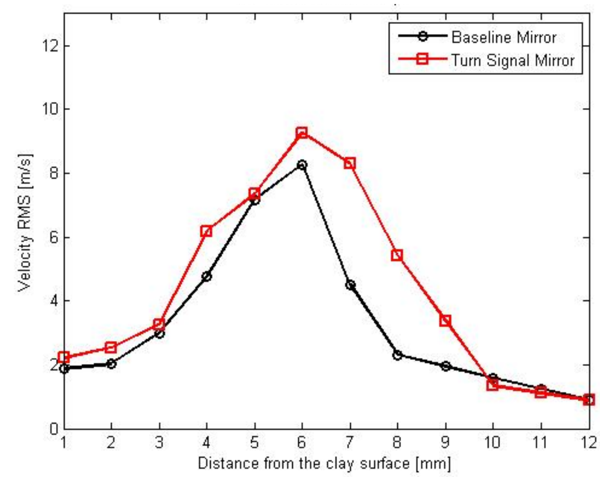

(b)

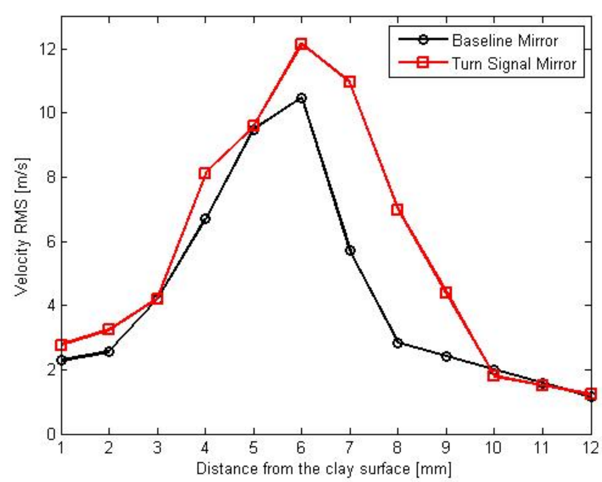

(c)

Figure 14
RMS velocity values for
(a) 25 m/s, (b) 33 m/s, (c) 42 m/s.

Table 1
RMS differences of three notable points
(Turn Signal RMS – Baseline RMS = RMS Difference)

Velocity (m/s)	6 mm away from clay surface [m/s]	7 mm away from clay surface [m/s]	8 mm away from clay surface [m/s]	Average RMS of three points [m/s]
25	0.53	2.65	1.78	1.65
28	0.68	3.10	2.32	2.03
31	0.86	3.54	2.47	2.29
33	1.00	3.79	3.10	2.63
36	1.14	4.22	3.34	2.90
39	1.36	4.87	3.94	3.39
42	2.15	5.24	4.14	3.85

Figures 15 through 20 show cross-correlations between Y-axis laser vibration measurements and hotfilm measurements for three different locations throughout the hotfilm probe measurement range (1, 6 and 12 mm away from the surface). The Δt on the x-axis indicates the amount of relative phase shift between the correlated records. The first set of three figures belongs to the baseline mirror. At a distance of 1 mm above the surface (Figure 15), the correlation values are relatively low for all phase shifts. However, at a distance of 6 mm above the mirror tip (Figure 16), the cross-correlation yields a peak value of 0.15, only for positive values of Δt, indicating that the wake structure is responsible for the mirror vibrations. Also, the peak values in the cross-correlation repeat every 22 ms of phase shift, indicating that a wake structure with a characteristic frequency of about 45 Hz is responsible for the mirror vibrations. At a probe location of 12 mm above the mirror tip (Figure 17), correlation between vibrations and the velocity data remains for positive values of Δt, but is diminished. Cross-correlations for the turn signal mirror (Figure 18 through Figure 20) show similar behavior, although the magnitude of the correlations continues to increase as the probe distance from the tip increases to 12 mm. This result indicates that the turn signal mirror has a wider wake than the baseline mirror. Thus, the cross-correlation data for both mirror configurations clearly indicates that unsteadiness in the wake with a characteristic period of 22 ms is responsible for the mirror vibrations. The level of correlation between vibrations and flow oscillations is approximately the same for both mirrors. However, since the flow unsteadiness for the turn signal mirror is significantly higher, the vibrations for that mirror geometry will also be higher.

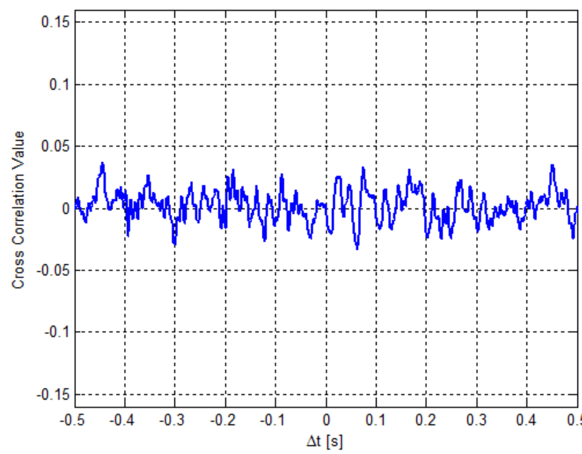

Figure 15
Cross-correlation between Y-vibration and hotfilm data for the probe 1 mm away from the surface for BL mirror

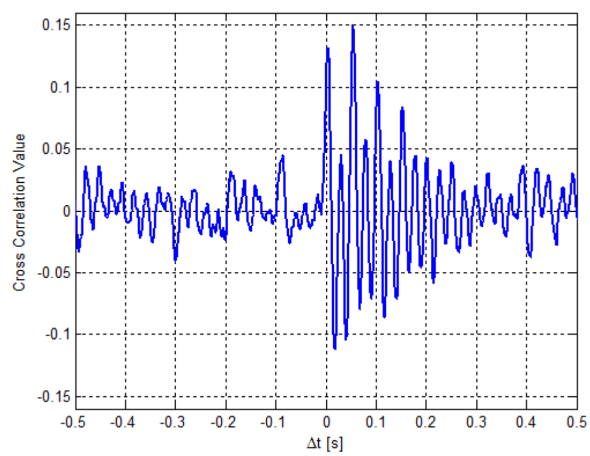

Figure 16
Cross-correlation between Y-vibration and hotfilm data for the probe 6 mm away from the surface for BL mirror

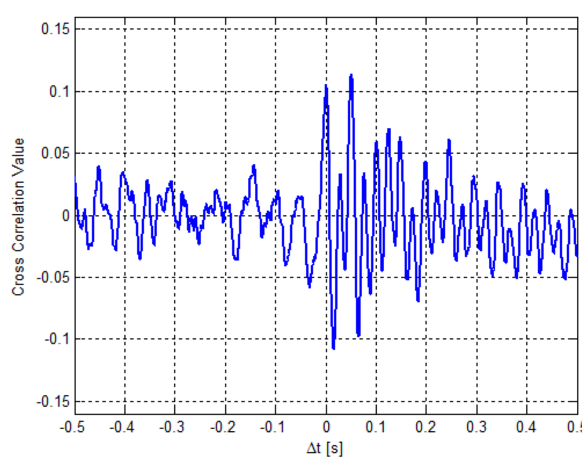

Figure 17
Cross-correlation between Y-vibration and hotfilm data for the probe 12 mm away from the surface for BL mirror

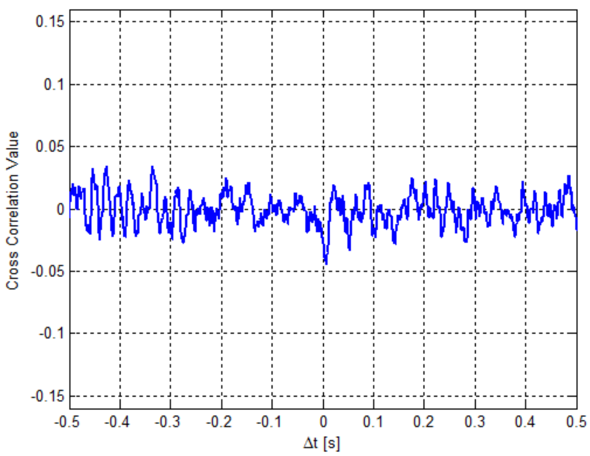

Figure 18
Cross-correlation between Y-vibration and hotfilm data for the probe 1 mm away from the surface for TS mirror

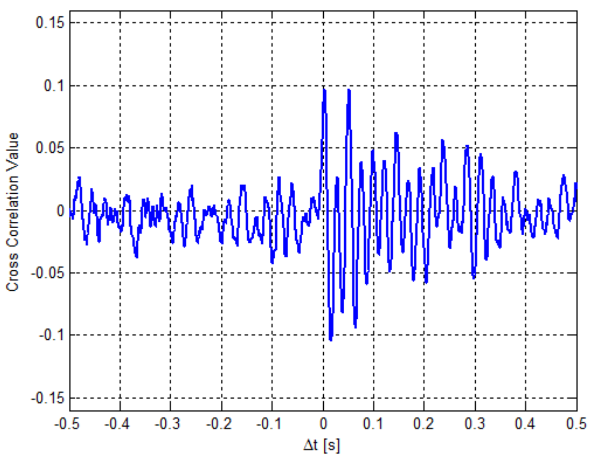

Figure 19
Cross-correlation between Y-vibration and hotfilm data for the probe 6 mm away from the surface for TS mirror

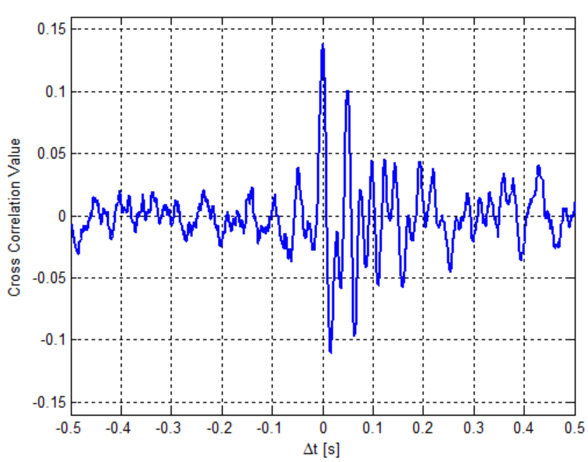

Figure 20
Cross-correlation between Y-vibration and hotfilm data for the probe 12 mm away from the surface for TS mirror

These hotfilm measurements helped to reinforce the conclusions derived from the PIV and flow visualizations, namely:

1. The separation location oscillates more for the flow over the turn signal mirror, and seems to be stable for the baseline mirror. This shifting in part causes unsteady aerodynamic loading on the mirror and exacerbates housing vibrations.

2. Tip modification of the baseline mirror causes a wider wake and higher levels of unsteadiness in the wake, which intensifies vibrations of the mirror housing.

Surface Stress Sensitive Film

Figure 21 shows one of the processed images obtained from the S^3F technique. The left section of this image is the measured surface shear stress field, while the right is the velocity profile. The top of the stress pattern image is upstream while the bottom is downstream. In the velocity profile, the blue line is the velocity magnitude. Note that it is negative on the top section, signifying a local velocity in the same direction as the free-stream, but then it shifts to a positive value, signifying a velocity in the opposite direction as the free-stream. In between this area, the separation occurs, and is shown by a dense grouping of lines pointing to the right on the stress profile. These results indicate a certain degree of spanwise uniformity of the separation line, and verify that flow separation occurs at the mirror tip where the geometry modification has been made.

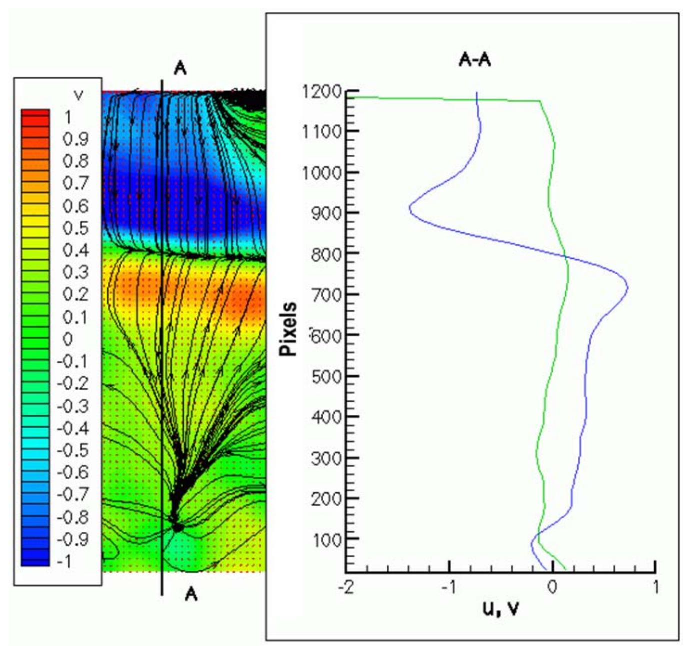

Figure 21
S^3F Image on the turn signal mirror supplied by Innovative Scientific Solutions Inc. (ISSI)

CONCLUSION

Flow-induced vibrations on two different side-view mirrors were investigated and compared. Vibrations were quantified by using a laser-based measurement technique. The turn signal mirror was found to have larger vibration magnitudes when compared to the baseline case. For higher velocities the difference in vibration magnitude between the two configurations becomes more distinguishable. The reason for the difference in vibrations was found to be rapid shifting of the separation location and wider wake on the turn signal mirror, due to the lack of a sharp edge that defines a separation location. Shifts in separation location and wake structure were clearly observed in flow visualization and PIV data. Velocity fluctuations, as a measure of unsteadiness, were also measured. Differences in RMS fluctuations in the wake and cross-correlations between vibrations and flow unsteadiness show that wake unsteadiness causes the vibrations. The curved tip modification on the turn signal mirror changes the flow characteristics and induces more unsteadiness in the flow resulting in worse vibration levels.

ACKNOWLEDGMENTS

The authors would like to thank Dr. Sergey Fonov and Dr. Jim Crafton from Innovative Scientific Solutions Inc. (ISSI) for their support in implementing the S^3F technique. The authors also express their gratitude to Marco Palacio and Riley Vollmer who assisted in the initial effort to set up this investigation.

REFERENCES

1. Achenbach, E., "Vortex Shedding from Spheres," *J . Fluid Mech.*, vol. 62, part 2, pp. 209-221, 1974.
2. Watkins, S., "On the Causes of Image Blurring in External Rear View Mirrors," SAE 2004-01-1309, *Society of Automotive Engineers*, SP-1874, pp. 401-410, 2004.
3. Horinouchi, N., Kato, Y., Kondoh, T., Yamada, T., and Ninomiya, O., "Development of Estimation Technique for Flow-Induced Vibration on External Rearview Mirror," SAE 2003-01-2815, *Society of Automotive Engineers*, 2003.
4. Homsi, E., and Narain, M., "Vibration Control of Body-Mounted Plastic Mirror Design," SAE 982312, *Society of Automotive Engineers*, 1998.
5. Tarasov, V.N., and Orlov, A.A., "Method for Determining Shear Stress on Aerodynamic Model Surface," Patent of Russia, 4841553/23/1990.
6. Fonov, V., Fonov, S., Jones, G., Crafton, J., "Image Processing Technique for Shear Stress Optical Measurements," *11th International Symposium On Flow Visualization*, University of Notre Dame, Notre Dame, Indiana, August 9-12, 2004.
7. Crafton, J.W., Fonov, S., Jones, E.G., Goss, L.P., Forlines, R.A., Fontaine, A., "Measurements of skin friction in water using surface stress sensitive films," Meas. Sci. Technol. **19**-75801, 2008.